3-2020

Non-linear Statistical Photocalibration of Photodetectors without Calibrated Light Sources

Stephen C. Cain
Air Force Institute of Technology

Recommended Citation

Stephen C. Cain, "Non-linear statistical photocalibration of photodetectors without calibrated light sources," Appl. Opt. 59, 2767-2775 (2020). https://doi.org/10.1364/AO.385753

Accepted Author Manuscript

Journal:	*Applied Optics*
Article Title:	Non-linear statistical photocalibration of photodetectors without calibrated light sources
Authors:	Stephen C. Cain
Accepted for publication:	18 February 2020
Final version published:	18 March 2020
DOI:	https://doi.org/10.1364/AO.385753

Non-Linear statistical photo-calibration of photodetectors without calibrated light sources

Stephen C. Cain
Air Force Institute of Technology, Department of Electrical and Computer Engineering, 2950 Hobson Way, Wright-Patterson AFB, OH, 45433

Abstract. Calibration of CCD arrays is commonly conducted using dark frames. Non-absolute calibration techniques only measure the relative response of the detectors. For absolute calibration to be achieved, a second calibration is sometimes utilized by looking at sources with known radiances. A process like this can be used to calibrate photodetectors if a calibration source is available and sensor time can be spared to perform the operation. A previous attempt at creating a procedure for calibrating a photodetector using the underlying Poisson nature of the photo-detection statistics relied on a linear model. This effort produced the SANUC (Statistically Applied Non-Uniformity Calibration) algorithm, which demonstrated an ability to relate the measured signal with the true radiance of the source.

Reliance on a completely linear model does not allow for non-linear behaviors to be described, thus potentially producing poor photo-calibration over large dynamic ranges. In this paper, a photo-calibration procedure is defined that requires only first and second moments of the measurements and allows the response to be modeled using a non-linear function over the dynamic range of the detector. The technique is applied to image data containing a light source measured with different integration times showing that the non-linear technique achieves significant improvement over the linear model over a large dynamic range.

Keywords: Calibration, Detection, Statistical Optics

Stephen C. Cain, E-mail: Stephen.Cain@afit.edu

1 Introduction

A new method of achieving non-uniformity correction for radiometric calibration of photodetectors is developed and tested in this research. The proposed algorithmic refinement allows radiometric quantification of the data in terms of electron count without substantial additional computational burden over a larger range of light levels than what is possible with the employment of methods that utilize photodetector statistics with a linear model to achieve calibration like "the variance method" and the S3NUC and SANUC algorithms. [1] [2] [3]. This is achieved with the introduction of a new non-linear model for the detector that determines photodetector response with only two parameters.

While it is recognized that photodetectors do not exhibit a linear response in [4], there are plenty of examples of successfully modeling them as such [5], [6], [7] when input signals are held over a small enough range. The variance, SANUC and S3NUC methods all require at least two sufficiently static datasets of the same scene at different integration times [1], [2] [3] in order to facilitate the calculation of calibration parameters. Other techniques have been introduced for achieving non-uniformity correction [5], [6], [7] , but these methods do not allow for absolute radiometry in terms of measured electrons to be achieved

without the addition of a calibrated light source. These methods allow for the non-absolute pixel-to-pixel differences in photo-detector response to be removed, but do not provide an estimate of the gain of the system in units of digital counts per electron or the bias in the linear model that allows the true number of photons to be estimated from the detector measurement and knowledge of the quantum efficiency and dark current level. Absolute radiometry was demonstrated with the SANUC method, but often the system response of a photodetector is not linear over its whole input range. The SANUC method is designed to fit the calibration of a non-linear detector to a linear detector response [2]. The introduction of a non-linear model that achieves an improved ability to describe the photo-detector response over the SANUC approach is the goal of this research.

The remainder of this paper is organized as follows: Section 2 provides an overview of the variance method and the SANUC algorithm. Section 3 will introduce and provide derivations for the Non-Linear Statistical Non-Uniformity Correction (NLSNUC) algorithm. Section 4 will serve to present the laboratory data and results that serve to compare the variance method, and the SANUC and NLSNUC algorithms by calibrating the detectors in an array of photo-detectors using two data sets and then using the calibration information to predict the system response for inputs outside the calibration range.

2 Variance Method and the SANUC Algorithm

The variance method can be used to compute the photo-detector gain and is identified and mathematically justified in [1]. This method features an approach of measuring the variance and mean of different data sets at different illumination levels. The method then specifies that the variance at each data point should be plotted against the mean. When this is accomplished for at least two data sets, but preferably more, a line can be fitted between the points and the slope of that line reveals the gain of the system in units of digital counts per electron. When more points are used, a more refined estimate of the gain may be produced. Using this technique, the y-intercept of the graph is the readout noise variance present even when there is no illumination on the photo-detector surface. No solution for the average number of electrons is presented using this method nor does this method offer a solution for detector bias. It is assumed that the photo-detector bias can be measured using dark frames.

The SANUC algorithm defines $\bar{K}(x,y)$, as the average number of electrons expected in the first data set (D_1). The average number of electrons measured in the second data set, (D_2), should be $N\bar{K}(x,y)$. In practice, this increase of the electron count can be readily accomplished by increasing the integration time of the sensor being used to gather the data by a factor of N [2].

Expressions for the mean, E[ ], and variance of the two sets of data , $D_1$and D_2, at pixel location (x,y) needed to calculate the linear detector parameters are shown in Equations (1-4) below:

$$\bar{D}_1(x,y) = E[D_1(x,y)] = G(x,y)\bar{K}(x,y) + B(x,y) + O \tag{1}$$

$$\bar{D}_2(x,y) = NG(x,y)\bar{K}(x,y) + B(x,y) + O \tag{2}$$

$$\sigma^2_{D_1}(x,y) = E[(D_1(x,y) - \bar{D}_1(x,y))^2] = G^2(x,y)\bar{K}(x,y) + \sigma_n^2 \tag{3}$$

$$\sigma^2_{D_2}(x,y) = NG^2(x,y)\bar{K}(x,y) + \sigma_n^2 \tag{4}$$

In these equations the digital offset, O, can be verified by setting the integration time of the camera to be as small as possible and closing the aperture to prevent any light from entering. With some equipment, this offset level can be selected by the user. This system of equations is then solved for the parameters *G* (the gain), *B* (the model bias), $\bar{K}$, and σ_n^2 (the variance of the readout noise) using estimates of the means ($\bar{D}_1, \bar{D}_2$) and variances ($\sigma^2_{D1}, \sigma^2_{D2}$) of the data sets D_1 and D_2. In Equation (5) the solution for the Gain is solved for as a difference of variances of the data set over the differences in the means between two data sets. This difference of variances in the numerator removes any common readout noise variance between the data sets.

$$G(x,y) = \frac{\sigma^2_{D_2}(x,y) - \sigma^2_{D_1}(x,y)}{\bar{D}_2(x,y) - \bar{D}_1(x,y)} \tag{5}$$

The solution for $\bar{K}$ shown in Equation (6) is a function only of the means of the two data sets and the estimated gain from Equation (5).

$$\bar{K}(x,y) = \frac{\bar{D}_2(x,y) - \bar{D}_1(x,y)}{(N-1)G(x,y)} \tag{6}$$

The calculation of the bias, *B*, is conducted using only the mean of one data set and the estimated gain and electron value.

$$B(x,y) = \bar{D}_1(x,y) - G(x,y)\bar{K}(x,y) - O \tag{7}$$

The SANUC method allows for the calculation of the gain in units of digital counts per electron and the "model bias", B, which can alternatively include the offset, O as it was originally presented in [2].

When the number of data sets is equal to two, the gain computed using the variance method is mathematically equivalent to the gain computed using the SANUC method. The slope would be rise over run, which is the difference between the two variances divided by the difference between the two means, as shown in Equation (5). Calculation of the variances removes the mean and any biases from the calculation as variance calculation dictates that you subtract the mean from the samples. The differences between the means in the denominator also subtracts any bias effects so that neither the model bias nor the voltage offset show up in a plot of variance versus signal mean as shown in Figure 1. If the system is completely linear, then the y-intercept is related to the observed readout noise variance, which is not equal to either the model bias or the voltage offset. Any error in the location of the y-intercept would be due to the non-linearity of the response and noise.

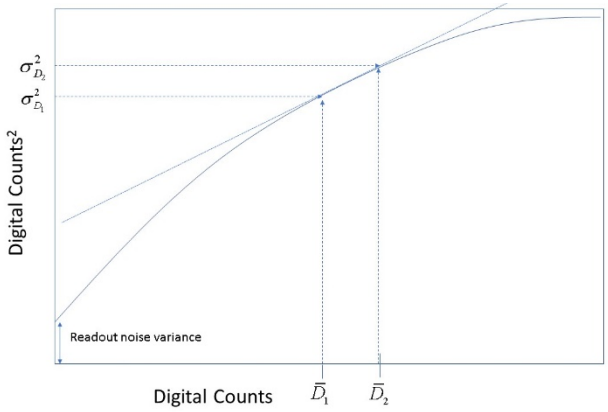

Figure 1: Employment of the variance method for a non-linear photodetector. The gain in units of digital counts per electron is the slope of the line tangent to the solid signal variance versus mean signal curve.

It is worth noting that the variance method offers no formal solution for $\bar{K}$ or the "model bias." It stands to reason that Equation (6) could be used to compute $\bar{K}$ using the calculated gain since two data sets are presumed to be available. The variance method assumes that the dark level (digital counts measured from dark frames with the same integration time as the illuminated data, but with no illumination) accounts for any bias. This would be true if the system response were completely linear. However, for non-linear systems, the dark level does not account for what this paper refers to as the "model bias."

Figure 2 shows a notional response curve that highlights the difference between the two quantities. Here the means are preserved because we are plotting average digital count on the y-axis versus photon input on the x-axis. The

signal mean is computed as a function of the number of electrons hitting the detector as part of the SANUC algorithm, but this calculation is not considered as part of the variance method. This is why the variance method cannot compute "model bias". The offset, O, is the signal measured with no input. More detailed information on the SANUC algorithm and its demonstrated radiometric accuracy can be found in [2].

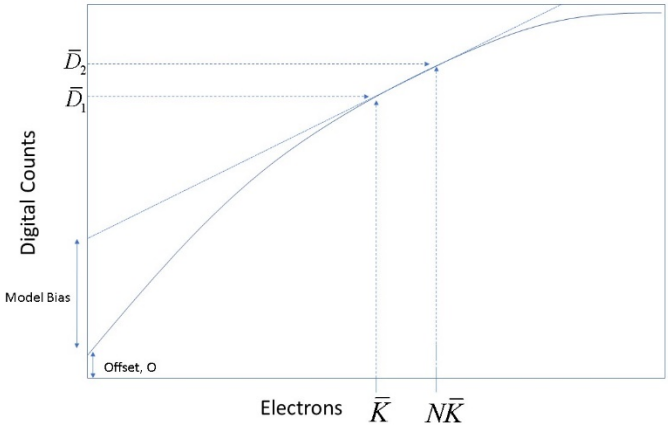

Figure 2: SANUC method showing how the model bias is computed from the graph of the system output versus input electrons.

3 Non-Linear Statistical Non-Uniformity Calibration (NLSNUC) Algorithm

The NLSNUC algorithm represents a further modification of the SANUC approach. The derivation of the approach is rooted in a hypothesis that the efficiency of a CCD element is a non-linear function of the number of electrons in the well. CCD wells are like capacitors in that they store charge. The energy required to add additional charge to an already charged capacitor is more than the energy required to add charge to a depleted capacitor. This increase in energy required for charging as the well fills produces a reduction in efficiency as a function of well occupancy, which should lead to a reduction in the system gain as the well becomes full. The hypothesized model relating the photo-detector output, D_N, in relation to the number of electrons measured by the detector during the integration time is shown in Equation (8).

$$D_N(x,y) = C(x,y)(1-e^{-\alpha(x,y)K(x,y)}) + O \tag{8}$$

In the experiments presented in the next section, the measurements were used to verify that the camera black level setting (what the user inputs for the black level) is indeed accurate. α is the non-linear gain factor of the camera pixel at location (x,y), N is the integration time factor (much the same as in the SANUC method) and *C(x,y)* is the pixel saturation value in units of digital counts. Since O is easily verified through a zero illumination measurement, and can be directly programed by the user and is

often independent of pixel elements (since it is driven by the output amplifier level relative to the analog to digital converter), the model possesses the same number of variables as the traditional linear model used by the SANUC method. Additionally, when the programmable offset, O, is removed, this model features the output of the camera being equal to the zero mean readout noise when there is no illumination present.

Calculation of model parameters for the NLSNUC algorithm is a two-step process. The same sort of calibration data is used for NLSNUC as in the variance and SANUC methods. A number of frames of data are collected while the light level presented to the detector array does not change. There is no need for the light level to be uniform across the array. First, the expected value of the two data sets are taken as shown in Equations (9) and (10).

$$E[D_{N_1}(x,y)-O] = C - CE[e^{-\alpha(x,y)K_1(x,y)}] \tag{9}$$

$$E[D_{N_2}(x,y)-O] = C - CE[e^{-\alpha(x,y)K_2(x,y)}] \tag{10}$$

In these equations, K_1 and K_2 are Poisson random variables with the mean of K_2 electrons being equal to the mean of K_1 times N_2 / N_1.Using the Moment Generating Function of a Poisson random variable [8], the ratio of Equation (10) divided by Equation (9) is equal to:

$$\frac{\bar{D}_2(x,y)}{\bar{D}_1(x,y)} = \frac{E[D_{N_2}(x,y)-O]}{E[D_{N_1}(x,y)-O]} = \frac{1-e^{N_2\bar{K}(x,y)(e^{-\alpha(x,y)}-1)/N_1}}{1-e^{\bar{K}(x,y)(e^{-\alpha(x,y)}-1)}} \tag{11}$$

Defining the variable *g(x,y)* being equal to the argument of the exponent in the denominator of Equation (11), this expression becomes:

$$\frac{\bar{D}_2(x,y)}{\bar{D}_1(x,y)} = \frac{1-e^{N_2 g(x,y)/N_1}}{1-e^{g(x,y)}} \tag{12}$$

The sample mean of D_{N2} divided by the sample mean of D_{N1} can be computed from the data to allow for *g(x,y)* to be estimated by finding the *g(x,y)* that minimizes the following equation.

$$\hat{g}(x,y) = \arg\min_{g(x,y)} \left(\frac{\bar{D}_2(x,y)}{\bar{D}_1(x,y)} - \frac{1-e^{N_2 g(x,y)/N_1}}{1-e^{g(x,y)}} \right)^2 \tag{13}$$

The estimate, $\hat{g}$, can be found through a numerical procedure of computing the quantity in Equation (13) for a range of values of *g(x,y)*. With this estimate for *g(x,y)*, it is possible to estimate *C(x,y)* by equating Equation (9) with $\bar{D}_1$ from Equation (11) and solving for *C(x,y)*.

$$C(x,y) = \bar{D}_1(x,y) / (1 - e^{\hat{g}(x,y)}) \tag{14}$$

With a solution of *C(x,y)* in hand, it becomes possible to transform the data sets D_{N2} and D_{N1} into two new data sets H_{N2} and H_{N1} respectively via the following equation:

$$H_N(x,y) = -\log(1 - (D_N(x,y) - O) / C(x,y)) \tag{15}$$

Following this transformation, H_N is now a random variable with mean equal to:

$$E[H_N(x,y)] = \alpha(x,y) N \bar{K}(x,y) \tag{16}$$

In this way, the non-linear calibration becomes a linear calibration problem where the model parameter *α(x,y)* takes on the role of the gain and the model bias is known to be zero. Thus, the SANUC algorithm can be used on the new data sets H_{N2} and H_{N1} to solve for the number of electrons and the gain. Table 1 shows the steps involved in how the different algorithms process laboratory data to compute calibration parameters and average photon rates.

Table 1: Steps in the variance method as well as the SANUC and NLSNUC Algorithms. The last row shows how to take the calibration parameters and compute an estimated number of electrons for each data sample. The term "Linear algorithms" refers to both the variance method and the SANUC algorithm when indicating the step number in column 1.

Step#	The variance method and SANUC	NLSNUC
Compute Offset, O 1 Linear algorithms 1 NLSNUC	O = Camera Black Level set by user (Can also be determined by dark frame measurements)	O = Camera Black Level set by user (Can also be determined by dark frame measurements)
Compute mean of data sets D_1, D_2 2 Linear algorithms 2 NLSNUC	Average the data in the frame dimension after subtracting the offset O	Same as SANUC
Compute variances of data sets D_1,D_2 3 Linear algorithms N/A NLSNUC	For each pixel in the array, compute the variance	Not done with NLSNUC
Compute detector gain 4 Linear algorithms 7 NLSNUC	$G(x,y)=\frac{\sigma^2_{D_2}(x,y)-\sigma^2_{D_1}(x,y)}{\bar{D}_2(x,y)-\bar{D}_1(x,y)}$	$\alpha(x,y)=\frac{\sigma^2_{H_2}(x,y)-\sigma^2_{H_1}(x,y)}{\bar{H}_2(x,y)-\bar{H}_1(x,y)}$
Compute $\bar{K}$ 5 Linear algorithms 8 NLSNUC	$\bar{K}(x,y)=\frac{\bar{D}_2(x,y)-\bar{D}_1(x,y)}{(N-1)G(x,y)}$	$\bar{K}(x,y)=\frac{\bar{H}_2(x,y)-\bar{H}_1(x,y)}{(N-1)\alpha(x,y)}$
Compute Model Bias 6 Linear algorithms N/A NLSNUC	Not done for the variance method For the SANUC algorithm: $B(x,y)=\bar{D}_1(x,y)-G(x,y)\bar{K}(x,y)$	Not necessary for NLSNUC
Compute the parameter $\hat{g}$ N/A Linear algorithms 3 NLSNUC	Not necessary for the variance method or SANUC	Numerical procedure of finding the value of $\hat{g}$ $\hat{g}(x,y)=\arg\min_{g(x,y)}\left(\frac{\bar{D}_2(x,y)}{\bar{D}_1(x,y)}-\frac{1-e^{N_2 g(x,y)/N_1}}{1-e^{g(x,y)}}\right)^2$
Compute the Saturation, C(x,y) N/A SANUC 4 NLSNUC	Not necessary for the variance method or SANUC	$C(x,y)=\sum_{f=1}^{M}\bar{D}_1(x,y)/(1-e^{\hat{g}(x,y)})$
Non-Linear Correction N/A Linear algorithms 5 NLSNUC	Not necessary for the variance method or SANUC	$H_1(x,y)=-\log(1-(D_1(x,y)-O)/C(x,y))$ $H_2(x,y)=-\log(1-(D_2(x,y)-O)/C(x,y))$
Compute means and variances of data with Non-Linear Correction N/A Linear algorithms 6 NLSNUC	Not necessary for the variance method or SANUC	$\bar{H}_1(x,y)=E[H_1(x,y)]$ $\bar{H}_2(x,y)=E[H_2(x,y)]$ $\sigma^2_{H_1}(x,y)=E[(H_1(x,y)-\bar{H}_1(x,y))^2]$ $\sigma^2_{H_2}(x,y)=E[(H_2(x,y)-\bar{H}_2(x,y))^2]$
Compute estimated value of K from data sample 7 Linear algorithms 9 NLSNUC	$\widehat{K}$ is an estimate of th number of electrons For the variance method: $\hat{K}(x,y,f)=(D(x,y,f)-O)/G(x,y)$ For SANUC: $\hat{K}(x,y,f)=(D(x,y,f)-B(x,y)-O)/G(x,y)$	$\widehat{K}$ is an estimate of the number of electrons $\hat{K}(x,y,f)=-\log(1-(D(x,y,f)-O)/C(x,y))/\hat{\alpha}(x,y)$

4 Demonstration of the NLSNUC algorithm

The calibration algorithms are evaluated using measured photo-detector data. In setting up the laboratory experiment, the goal was to present a steady intensity pattern on the detector array so that measurements at different integration times could be related to one another without concern that the source was changing in intensity. For this reason, a 4.5-volt DC lamp was powered by 3 AA batteries to flood-illuminate a white board which then reflected light onto the detector array. Sets of data were taken with the CCD (Charge Coupled Device) array covered (no light) as well as exposed to the reflected light with exposures of 1ms, 2 ms, 20 ms, 40 ms, and 100 milliseconds. Figure 3 shows the laboratory setup.

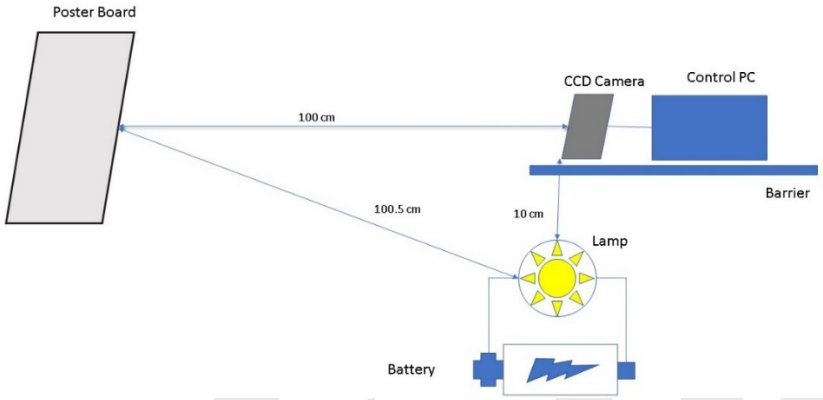

Figure 3: Laboratory setup showing the relationship between the lamp, CCD array and reflective surface.

The 40 and 100 ms exposure data are used to compute the calibration parameters as well as estimate the number of electrons being measured during a 1 ms period using the procedures outlined in the previous sections. These model parameters are then used to compute the predicted number of digital counts produced during the 1 ms, 2 ms and 20 ms integration periods. The methodology used for comparison of the algorithms involves processing sets of data as described in Table 1. Each set of data is taken with different integration times (1ms, 2 ms, 20ms, 40 ms, 100ms) and contains ten-thousand photo-detectors (100 by 100 area of the detector) each of which collected 100 samples in time of the intensity of the field incident on their surface. Table 2 summarizes the collection parameters. The "Dark" data set was used to verify the digital bias of the CCD array of 52 digital counts and closely represents the output of the camera when there is no light incident on the CCD surface. Further experiments showed that for all integration times, the dark level (camera output with no light present) was 52 digital counts. This allows for the conclusion that this camera has a dark current of less than 10 electrons/second.

Table 2: Data sets and Integration Times

Data Set	Integration Time (milliseconds)	Median Digital Count
Dark	1, 2, 20, 40 and 100	52
D_1	1	188
D_2	2	309
D_{20}	20	2400
D_{40}	40	4704
D_{100}	100	11215

Figure 4 shows a sample image gathered by the ThorLabs 8050M scientific camera used to collect the data for these experiments. It has a thermo-electric cooler which helps control the readout noise present in the image data to a level of 10 electrons (root means squared). The pixel pitch is 5.5 micro-meters and the array size is 2472 by 3296 pixels. The camera digitizes the output using 14 bits of resolution. [9]

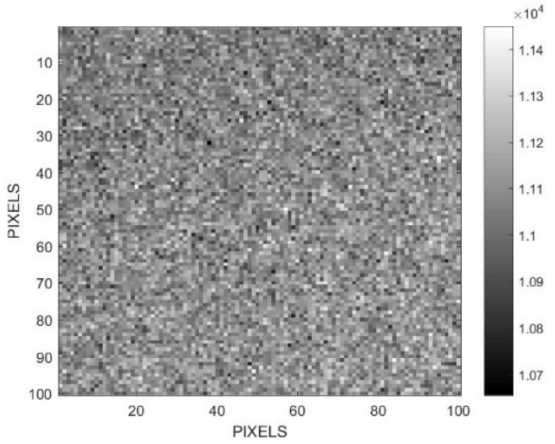

Figure 4: 100 by 100-pixel image of a flat field collected with the ThorLabs 8050M Scientific grade CCD camera. This image was gathered with an integration time of 100 ms and the region of interest (100 by 100 pixels) was chosen to speed up the image acquisition process and decrease processing time.

Figure 5 shows a flow chart for the processing steps showing how the results are obtained.

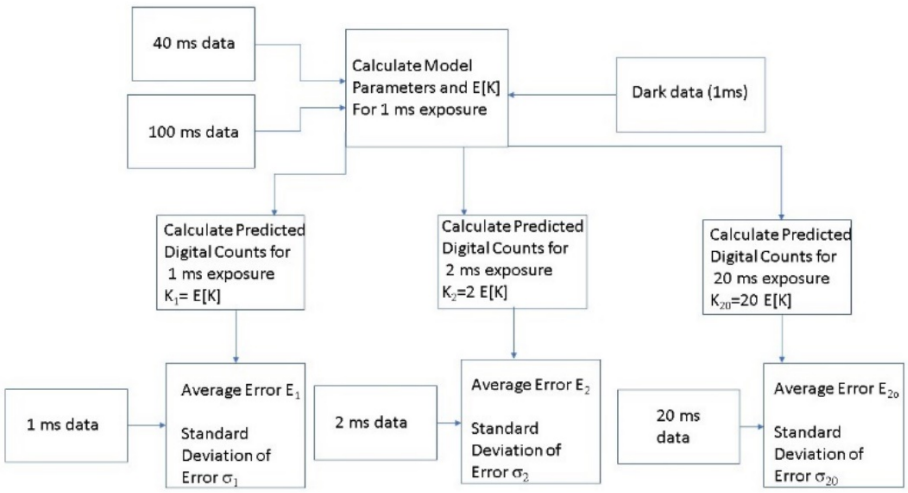

Figure 5: Flowchart showing how laboratory data is analyzed to produce estimates of calibration error.

The model parameters are then used to predict the photo-detector response to another input, which is then compared to a photo-detector response not used in the calibration. In this way, the superior calibration technique can be ascertained by determining which technique provided the better parameters for predicting the photo-detector response to an input outside the range of those used for calibration (the 40 and 100 ms data sets).

One hundred samples of 40 ms and 100 ms integration time data are used to compute, $\overline{K}$, a gain G, and bias B using the variance method and the SANUC algorithm. The median values of the parameters estimated over 10,000 photodetectors (100 samples per detector) are shown in Table 3.

Table 3: Median values for the estimates from the variance method calibration and the SANUC calibration using 40 and 100 ms data sets.

Parameter	Value	Unit
$\overline{K}_1$	443.42	Electrons
Gain (G)	0.1687	Digital Counts/Electron
Bias (B)	Not computed for the variance method 201.975 for SANUC	Digital Counts

Similarly, the 40 ms and 100 ms data were used to calculate the model parameters using the NLSNUC algorithm for each of 10,000 pixels using 100 samples per photodetector. Median values for the NLSNUC parameters over the 10,000 photodetectors (100 samples per detector) are shown in Table 4.

Table 4: Median values for the estimates from NLSNUC calibration using 40 and 100 ms data sets.

Parameter	Value	Unit
K_1	391.84	Electrons
Nonlinear Gain (α)	2.366×10^{-6}	$Electrons^{-1}$
Saturation Parameter (C)	1.0277×10^{5}	Digital Counts

Figure 6(A) shows the distributions for the gain parameter obtained from the variance method and the SANUC algorithm. Some of the values are negative, which demonstrates the method is susceptible to noise.

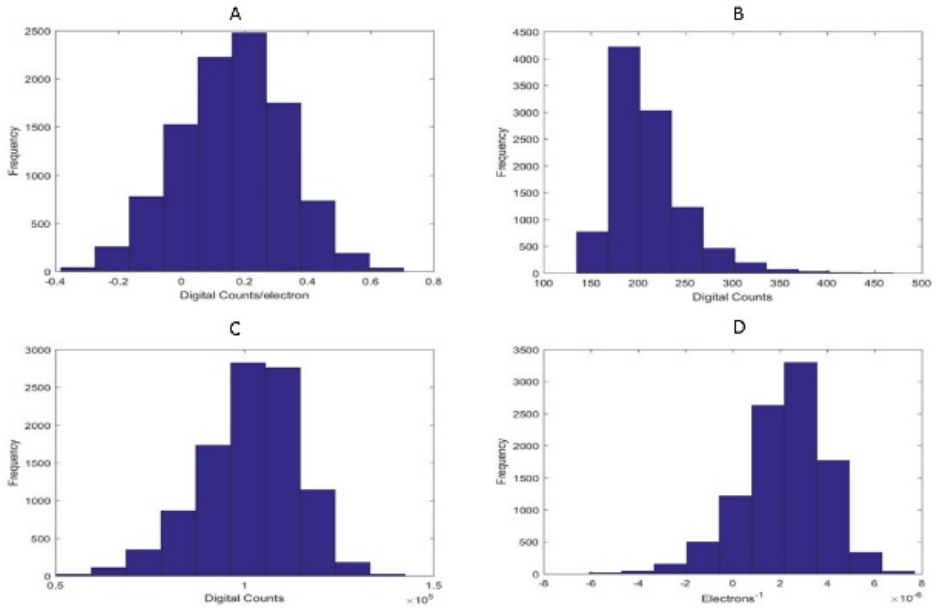

Figure 6: (A) Histogram of the gain computed by the variance method and the SANUC algorithm of the 10,000 photodetectors showing a standard deviation of the gain of 0.168 digital counts per electron. 82.7% of the pixels have positive gain values. (B) Histogram of the bias computed by the SANUC algorithm of the 10,000 photodetectors showing a standard deviation of 38 digital counts. (C) Histogram of the saturation parameter computed by the NLSNUC algorithm of the 10,000 photodetectors showing a standard deviation of 12724 digital counts. (D) Histogram of the nonlinear gain computed by the NLSNUC algorithm of the 10,000 photodetectors showing a standard deviation of 1.76E-6 $electrons^{-1}$. 89.2 % of the pixels report positive gain values, which is 6.5% more than what the variance method and the SANUC algorithm achieved.

Figure 6(B) shows a histogram of the bias values obtained from the SANUC algorithm. Figure 6(C) shows the distribution of the saturation parameter computed using the NLSNUC algorithm. Figure 6(D) shows the nonlinear gain parameter computed by the NLSNUC algorithm. Although some of the gain values are negative, the percentage of negative ones is smaller than that generated by the variance method and the SANUC algorithm, thus demonstrating the superior robustness of the NLSNUC algorithm.

Table 5 shows the results of applying the variance method, as well as the SANUC and NLSNUC algorithms to the data over 10,000 pixels (each trial having 100 data samples) . Equation (17) shows how the mean absolute error, E_N, is computed, where N is the integration time in milli-seconds, L is the number of columns and rows in the square image and M is the number of frames of data. In this experiment L=100 and M=100.

$$E_N = \frac{\sum_{x=1}^{L}\sum_{y=1}^{L}\sum_{m=1}^{M} | D_N(x,y,m) - I_N(x,y) |}{ML^2} \tag{17}$$

In this equation, $I_N(x,y)$ is the predicted number of digital counts for data calculated with an integration time of N milliseconds from the calibration parameters and the estimated average number of electrons. $I_N(x,y)$ is computed from Equation (18) for measuring the performance of the variance method error, Equation (19) for the SANUC algorithm, and Equation (20) when computing the performance of the NLSNUC algorithm.

$$I_N(x,y) = G(x,y)N\bar{K}(x,y) + O \tag{18}$$

$$I_N(x,y) = G(x,y)N\bar{K}(x,y) + B(x,y) + O \tag{19}$$

$$I_N(x,y) = C(x,y)(1 - e^{-\alpha(x,y)N\bar{K}(x,y)}) + O \tag{20}$$

The accuracy of the algorithm is revealed by the mean absolute error. The statistical significance of the results can be determined by evaluating the variation of the mean absolute error over all detectors in the array compared to the differences in the error between the methods. The standard deviation of the absolute error, σ_N, can be computed via Equation (21) and has units of digital counts. The numerator of Equation 21 is the standard deviation of the error for a pixel element. Because the error, E_N,

represents an average of the errors in all pixels , the deviation of E_N is reduced by the square root of the number of pixels used in the calculation (factor of 100 reduction) due to averaging over many pixels.

$$\sigma_N = \sqrt{\frac{\sum_{x=1}^{L}\sum_{y=1}^{L}\sum_{m=1}^{M}\left(|D_N(x,y,m) - I_N(x,y)| - E_N\right)^2}{ML^2}} \Big/ L \tag{21}$$

The calibration algorithms' performance reported in Table 5 shows the performance for each algorithm for all the data sets gathered in the study. The minimum error difference reported in row 5 is the difference between the lower of the variance method or SANUC average errors and the NLSNUC error. Row 6 shows the ratio of the number reported in row 5 divided by the twice the largest error deviation computed from Equation (21) for all the methods used on that particular data set. This provides a lower bound on the ratio reported in row 6. The ratio appearing in row 6 of Table 5 gives an estimate of the number of standard deviations in the error difference. If the number of standard deviations is greater than 6, then the probability that the NLSNUC algorithm produces lower error than the next best competitor is greater than 99.9999%.

Table 5: Laboratory results for all calibration algorithms with all units in digital counts. The error difference and % Confidence rows are only applicable for the error columns and not the deviations.

Algorithm	E_1	E_2	E_{20}	E_{40}	E_{100}	σ_1	σ_2	σ_{20}	σ_{40}	σ_{100}
variance method	25.97	37.03	152.63	260.89	260.90	.02	.03	.19	.38	.43
SANUC	184.17	173.10	59.73	57.67	63.24	.37	.36	.19	.04	.05
NLSNUC	17.14	19.53	27.79	37.84	45.70	.01	.02	.02	.03	.08
Min Error Difference	8.83	17.50	31.94	19.83	17.54	N/A	N/A	N/A	N/A	N/A
$\frac{\min Err\ Diff}{\sqrt{2\sigma_N^2}}$	16.8	33.5	118.9	70.4	28.8	N/A	N/A	N/A	N/A	N/A
Confidence	>99.99%	>99.99%	>99.99%	>99.99%	>99.99%	N/A	N/A	N/A	N/A	N/A

These results demonstrate that the NLSNUC algorithm provides a much better fit to the data than either the variance method or the SANUC algorithm, even for the points used to perform the calibration, and that these results are statistically significant with

high confidence, since the separation in the error performance between the algorithms' computed error, E_N, is many times greater than the error standard deviations. Figure 7 shows the estimated response curves of the variance method, the SANUC algorithm and the NLSNUC algorithm. SANUC produces a response curve that matches the NLSNUC curve where the input is consistent with the 40 and 100 ms data sets used in computing the calibration parameters, while the variance method doesn't. This is due to the lack of "model bias" in the variance method. At the low end, the NLSNUC and the variance method agree more closely, because the offset in this range is more closely equal to the offset, O. Although the curves appear nearly linear, the NLSNUC has lower error in both the high and low regions due to its ability to "bend", where the other techniques cannot, as shown in Table 5.

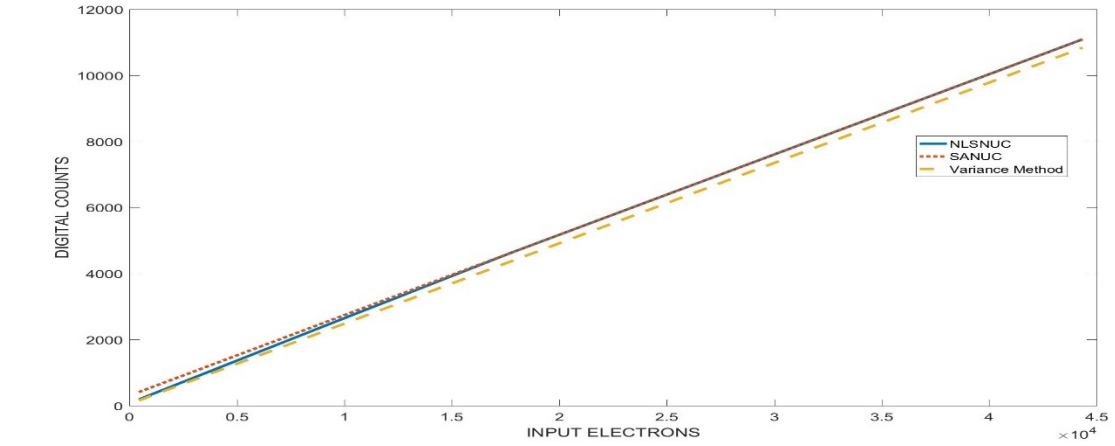

(A)

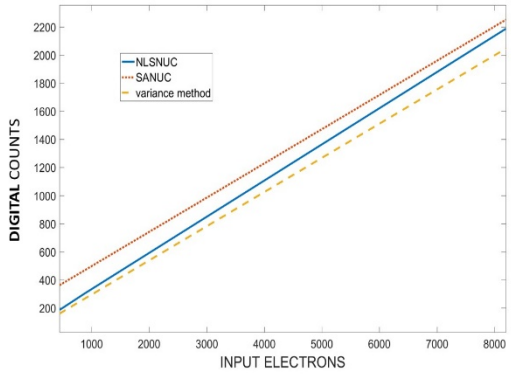

(B)

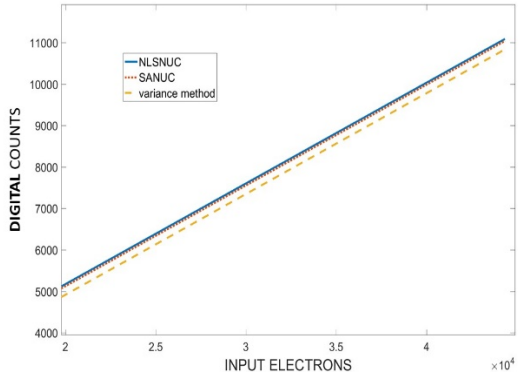

(C)

Figure 7: (A) Total estimated response curves for the three methods showing output digital counts vs. input electrons. (B) shows the low end of the range corresponding to inputs from the 1, 2 and 20 ms data sets. (C) shows the response curves in the high end corresponding to the 40 and 100 ms data sets used to calibrate the system.

5 Conclusions

The NLSNUC calibration algorithm produced superior performance well outside the calibration range of the experiment. This claim is based on the fact that the 40ms and 100ms integration time data were used to compute the calibration parameters and the calibration parameters were used to predict the response of the camera at integration times of 1,2 and 20ms for the same illumination level. The NLSNUC algorithm was the most accurate out of all the algorithms tested in the 1ms, 2ms and 20ms cases, which had illumination levels not found in the calibration data. The non-linear model utilized in the derivation of the new algorithm successfully modeled the response of the CCD pixels and has the feature that it is zero when the CCD pixels are not being illuminated and the offset, O, is subtracted along with any dark current.

This zero point provides the model an anchor near zero illumination that improves its performance over the linear model, which cannot guarantee that the response of the detector at zero illumination is in fact zero, due to model bias errors. The zero point effectively supplies a third data point in a two-point calibration that allows the NLSNUC algorithm to predict CCD output values more accurately than the linear model far from the calibration points. This is especially important if the system is calibrated at the high end of the response range. Extending the utility of the SANUC technique to a broader range of input makes the NLSNUC algorithm an important step forward in providing the ability to provide radiometric calibration of photodetectors without calibrated light sources.

Funding

Funding was provided by the Air Force Office of Scientific Research (AFOSR) JON 19ENG203

Disclosures

Any opinions expressed in this document are those of the author and do not necessarily represent those of the United States Air Force or the Department of Defense.

The author declares no conflict of interests.

References

[1] I. S. MacLean, Electronic Imaging in Astronomy, 2nd edition, pp. 321-323, Chickester: Praxis Publishing, 2008.

[2] N. J. Yielding, S.C. Cain, and M.D. Seal, "Statistical photocalibration of photodetectors for radiometry without calibrated light sources," *Optical Engineering,* vol. 57, no. 1, p. 10.1117/1.OE.57.1.014107, 2018.

[3] A. Catarius and M. Seal, "Static scene statistical algorithm for nonuniformity correction in focal-plane arrays," *Applied Optics,* vol. 54, no. 10, pp. 1-6, 2015.

[4] I. K. Baldry, *Time-Series Spectroscopy of Pulsating Stars,* pp. 33, Sydney: University of Sydney, 1999.

[5] J. G. Harris and Y.-M. Chiang, "Nonuniformity correction of infrared image sequences using the constant-statistics constraint," *IEEE Transations on image processing,* vol. 8, no. 8, pp. 1148-1151, 1999.

[6] M. M. Hayat, Sergio N. Torres, E. Armstrong, S. C. Cain and B. Yasuda, "Statistical Algorithm for Nonuniformity Correction in Focal Plane Arrays," *Applied Optics,* vol. 38, no. 5, pp. 772-780, 1999.

[7] R. C. Hardie, M. M. Hayat, E. Armstrong and B. Yasuda, "Scene-based nonuniformity correction with video sequences and registration," *Applied Optics,* vol. 39, no. 8, pp. 1241-1250, 2000.

[8] J. Goodman, Statistical Optics, pp. 37, New York: John Wiley & Sons, Inc, 1985.

[9] "Thor Labs 8050M-GE," Thor Labs, 2020.

Caption List

Figure 1: Employment of the variance method for a non-linear photodetector. The gain in units of digital counts per electron is the slope of the line tangent to the solid response curve.

Figure 2: SANUC method showing how the model bias is computed from the graph of the system output versus input photons

Figure 3: Flowchart showing how laboratory data is analyzed to produce estimates of calibration error.

Figure 4: 100 by 100 pixel image of a flat field collected with the ThorLabs 8050M Scientific grade CCD camera. This image was gathered with an integration time of 100 ms and the region of interest (100 by 100 pixels) was chosen to speed up the image acquisition process and decrease processing time.

Figure 5: Flowchart showing how laboratory data is analyzed to produce estimates of calibration error.

Figure 6: (A) Histogram of the gain computed by the variance method and the SANUC algorithm of the 10,000 photodetectors showing a standard deviation of the gain of 0.168 digital counts per electron. 82.7% of the pixels have positive gain values. (B) Histogram of the bias computed by the SANUC algorithm of the 10,000 photodetectors showing a standard deviation of 38 digital counts. (C) Histogram of the saturation parameter computed by the NLSNUC algorithm of the 10,000 photodetectors

showing a standard deviation of 12724 digital counts. (D) Histogram of the nonlinear gain computed by the NLSNUC algorithm of the 10,000 photodetectors showing a Standard deviation of 1.76E-6 electrons^{-1}. 89.2 % of the pixels report positive gain values, which is 6.5% more than what the variance method and the SANUC algorithm achieved.

Figure 7: (A) Total estimated response curves for the three methods showing output digital counts vs. input electrons. (B) shows the low end of the range corresponding to inputs from the 1, 2 and 20 ms data sets. (C) shows the response curves in the high end corresponding to the 40 and 100 ms data sets used to calibrate the system.

Table 1: Steps in the variance method as well as the SANUC and NLSNUC Algorithms. The last row shows how to take the calibration parameters and compute an estimated number of electrons for each data sample. The term "Linear algorithms" refers to both the variance method and the SANUC algorithm when indicating the step number in column 1.

Table 2: Data sets and Integration Times

Table 3: Median values for the estimates from the variance method calibration and the SANUC calibration using 40 and 100 ms data sets.

Table 4: Median values for the estimates from NLSNUC calibration using 40 and 100 ms data sets.

Table 5: Laboratory results for all calibration algorithms with all units in digital counts. The error difference and % Confidence rows are only applicable for the error columns and not the deviations.